JOURNAL OF CATALYSIS 133, 263–278 (1992)

Aluminum Coordination and Lewis Acidity in Transition Aluminas

F. R. CHEN, J. G. DAVIS, AND J. J. FRIPIAT[1]

Department of Chemistry and Laboratory for Surface Studies, University of Wisconsin, P.O. Box 413, Milwaukee, Wisconsin 53201

Received April 18, 1991; revised September 5, 1991

Besides the resonance lines attributable to tetrahedrally (Al^{IV}) and octahedrally (Al^{VI}) coordinated aluminum, the MAS NMR ^{27}Al spectra of transition aluminas obtained from finely divided precursors gibbsite and boehmite have a line which can be assigned to pentacoordinated Al (Al^{V}). This line which is very intense in ex-boehmite aluminas, as compared to ex-gibbsite aluminas, is also observed in the nonframework alumina moieties in acid and dealuminated zeolites. The isotropic chemical shifts of the Al^{VI}, Al^{V}, and Al^{IV} resonance lines are 11.4, 38.3 and 65.6 ppm, respectively, in a field of 11.77 T. Nutation (two-dimensional) spectra of ^{27}Al in these aluminas show a broad distribution of quadrupole coupling constants (QCCs) between ~2 and ~5 MHz. A broad range of distortions of the Al coordination shells corresponds to this range of QCCs. To detect electron acceptor sites (or Lewis acid centers), an EPR molecular probe has been adsorbed and the EPR spectra have been recorded before and after introduction of molecular oxygen. With dimethylaniline (DMA) the formation of a radical cation is observed and its concentration is larger on aluminas with Al^{V} than on aluminas without detectable Al^{V}. Molecular O_2, which is adsorbed on DMA-treated aluminas, acts as an electron scavenger picking up the electron transferred from DMA to the surface. Moreover, the g_{zz} is in the range expected for O_2^-, indicating its interaction with an Al nucleus. The surface density in electron acceptor sites with electron affinity ~ -7.1 eV is, at the best, on the order of 0.4×10^{12} spins/cm^2. These findings suggest either that strongly distorted shells of pentacoordinated Al are potential Lewis acid centers or that they generate such sites upon thermal activation. Other types of coordination, if sufficiently distorted, may play a similar role.

INTRODUCTION

Among the natural aluminosilicates, aluminum is, in most cases, either fourfold or sixfold coordinated (Al^{IV} or Al^{VI}, respectively). A few exceptions where aluminum is pentacoordinated (Al^{V}) are known, such as in andalusite (*1*). In this mineral the isotropic chemical shift (δ_{cs}) of the central transition of the ^{27}Al resonance is at 36 ppm with respect to a dilute solution of $Al^{3+}(6H_2O)$ (*2,3*) under magic angle spinning conditions (MAS). Depending upon the magnitude of the second-order quadrupolar shift (δ_{QS}) and of the bond angles, the center of gravity (δ_{CG}) of the resonance line of Al^{IV} is between 55 and 70 ppm, whereas that of Al^{VI} is between 0 and 11 ppm (*3*). In transition aluminas obtained through thermal decomposition of bayerite or boehmite, two broad lines at ~65 and ~8 ppm are observed in agreement with the pseudospinel structure assigned to these materials by Bragg (*4*) and Wells (*5*). As shown later the intensity ratio of these lines (Al^{IV}/Al^{VI}) is about 2, in agreement with the ratio of the numbers of tetrahedral to octahedral sites in a spinel. In well-crystallized zeolites, aluminum is tetrahedrally coordinated, with δ_{CG} between 55 and 65 ppm (*3*), but upon steaming and or dealumination, nonframework alumina species are formed and the ^{27}Al MAS NMR signal becomes more complicated. Besides the initial framework Al^{IV}, the nonframework aluminum shows resonance lines which could be assigned to Al^{VI}, Al^{IV}, and Al^{V} or to distorted Al^{IV} species (*7–11*) with δ_{CG} of about 5, 55–65, and 30–35 ppm, re-

[1] To whom correspondence should be addressed.

0021-9517/92 $3.00

spectively. In hydrated samples a narrow line at 0 ppm is often observed, suggesting the presence of some Al^{3+} cations balancing lattice charges.

^{27}Al signals with at least three lines have also been found in dehydroxylated kaolinite (metakaolinite) (*9–13*) and also in Al pillared silicic acid (*14*).

^{27}Al nutation experiments by Samoson *et al.* (*6*) suggest that in dealuminated Y zeolites the nonframework alumina species have strong quadrupolar interaction (~6 MHz), bringing about a large second-order quadrupolar shift. Their estimate of the quadrupole coupling constant (QCC) may be exaggerated because a distribution of sites within a range of QCCs is likely.

In alumina films obtained by anodic oxidation of aluminum foils, Dupree *et al.* (*15*) have also observed a line near 30 ppm that they assigned to Al^{V} in agreement with structural analysis by radial distribution function by Oka *et al.* (*16*). Another interesting observation has been reported by Paramzin *et al.* (*17*). Ground gibbsite, dehydroxylated at temperatures larger than 300°C, exhibits an ^{27}Al MAS NMR spectrum showing the resonance line at about 30 ppm (δ_{CG}), whereas this line is absent in the aluminas obtained from the unground precursor. Both materials, however, exhibit the Al^{IV} and Al^{VI} line at the usual frequencies. This observation tells us something important, namely, (i) the line at ~30 ppm can exist independently of those assigned to Al^{IV} and Al^{VI} and (ii) the appearance of this line seems connected to the particle size of the precursors before calcination. It could be speculated that if nonframework alumina is formed inside the zeolite structure, the particle size should be small enough to yield the line at 30 ppm, whereas alumina clusters formed outside zeolite framework can be large enough to prevent the formation of Al^{V}.

The relationship between Lewis acidity and the nature of the Al environment is of prime interest in acid catalysis and, to date, it is not known what kind of coordination is most likely to favor the formation of Lewis sites. Moreover, since a distribution of Lewis acid strengths is likely, it would also be most interesting to estimate, even in a qualitative way, the effect of the Al environment on the strength of the associated Lewis sites. In zeolites the difficulty of the problem is still aggravated by the often invoked, but never specified, synergy between Brønsted and Lewis acid sites.

Thus, a first step for solving the Lewis site problem would be to better understand the nature of transition aluminas with either two or three main kinds of Al coordination and see whether or not they have different Lewis acidities or different ranges of Lewis acid strengths. Thus, besides the MAS NMR techniques we suggest using an EPR technique to obtain information on the Lewis acidity. This technique is described elsewhere (*18,19*) and we will summarize briefly the main principles. Let A_L be the electron affinity of a Lewis site and let I_R be the ionization potential of a probe molecule liable to form a radical cation $R^{+\cdot}$. If the probe molecule when chemisorbed yields the radical cation spectrum, it means that $A_L < -I_R$ as required by the reaction

$$L + R \rightarrow L^{-} + R^{+\cdot}.$$

If, in addition, the exposure to O_2 increases the signal, it may be assumed that the pair LO_2^- is more stable than L^-. The electron affinity of $O_2 + e \rightarrow O_2^-$ is -0.44 eV. The affinity of L for O_2^- is not known. If it is large enough the EPR features of O_2^- should appear and it should eventually dominate over the $R^{+\cdot}$ spectrum. The EPR spectra of O_2^- have been reviewed by Che and Tench (*20*) and examples of O_2^- interacting with ^{27}Al nuclei are reported. Most often they have been observed on γ-irradiated zeolites or on alumina treated by N_2O (*21*). In both of these cases the g tensor is asymmetrical with g_{zz} with a value as large as 2.040. The value of $g_{xx} \simeq g_{yy} \simeq 2.006 \pm 0.002$. The formation of O_2^- on an aluminum site after interaction with aniline and the formation of the corresponding radical cation is reported

in Ref. (*19*). The interaction with the $I = 5/2$ nucleus is evidenced by the hyperfine splitting into six lines on dealuminated H-mordenite. The ionization potential of aniline is 7.7 eV. For weaker electron acceptor sites, as found in the present study, *N,N'*-dimethylaniline with a ionization potential of 7.1 eV is a more suitable probe.

A fundamental objection to the comparison between "structural" determination by ^{27}Al MAS NMR and the "surface" information obtained from the suggested EPR technique is that any relationship between both kinds of results cannot be more than circumstantial, the conclusions being based on related, but not direct evidences.

In fact, it is implicitly assumed that the bulk and surface structural features are related qualitatively. In a spherical particle with a 77-Å radius the percentage of Al contained in an outer layer 3 Å thick is about 11% and the corresponding surface area of 1 g of such particles (with density 3.9) is 100 m^2. It seems unlikely that one species of Al would be present solely in the core or in the outer layer, but it would be equally surprising if its bulk and surface concentrations would be the same. As shown later with the experimental conditions used here, most of the Al is seen. Since there is no reason to believe that the outer layer(s) of Al escapes detection, it is hoped that qualitative information can be obtained in characterizing aluminas by NMR and in studying their Lewis sites by an EPR molecular probe.

EXPERIMENTAL

Materials

The aluminum hydroxide precursors were obtained as follows. Gibbsite was prepared by boiling a 1 *M* $NaAlO_2$ solution for 1 day. The precipitate was washed carefully by centrifugation and identified by X-ray diffraction (XRD). Gibbsite was transformed into boehmite by hydrothermal synthesis at 350°C (5 g gibbsite + 10 ml water) and boehmite was identified also by XRD. Figures 1a and b show selected scanning electron micrographs of the starting materials. Gibbsite forms large well-defined crystals whereas boehmite consists of tiny layered crystals. Gibbsite was ground for more than 100 h in a ceramic ball mill either in the dry state or in the presence of water (Fig. 1c). Air-dried boehmite was ground for 350 h into small particles, as shown in Fig. 1d. Wet and dry grinding of gibbsite for the same time resulted in appreciably different particles sizes, dry grinding producing smaller particles than wet grinding. Dry grinding boehmite for 350 h achieved approximately the same particle size as grinding gibbsite for 100 h (compare Figs. 1c and 1d). Calcination does not affect the apparent particle size of the ground material. BET N_2 surface area measurements confirmed these observations. The surface of gibbsite was 6.5 m^2/g; wet-ground gibbsite had a surface area of 52 m^2/g and dry-ground gibbsite had a surface area of 163 m^2/g. Boehmite has a surface area of 9 m^2/g which increases to about 130 m^2/g upon dry grinding. Upon severe reduction of the particle size, the XRD of the precursor showed that amorphization had occurred to a large extent. Calcination of the precursors between 400 and 800°C produced X-ray amorphous aluminas whether they were ground or not. Their specific surface areas are shown in Table 1. Aluminas obtained with this procedure will be called either ex-gibbsite or ex-boehmite aluminas.

Techniques

^{27}Al NMR resonance. The samples used for the NMR study were not protected

TABLE 1

N_2BET Surface Areas (m^2/g) of Amorphous Aluminas Calcined for 1 h at the Indicated Temperature.

Precursor	Temperature (°C)		
	400	600	800
Gibbsite	168	172	—
Dry ground gibbsite	169	133	104
Boehmite	9	70	—
Dry ground boehmite	126	104	116

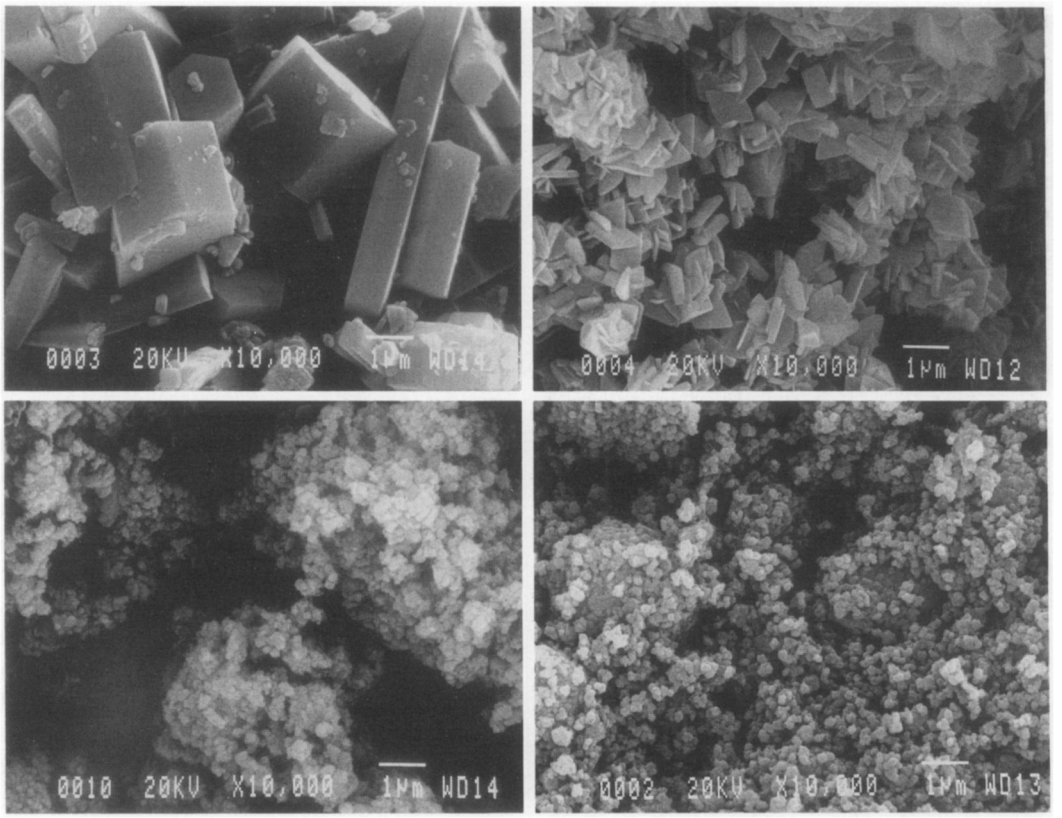

FIG. 1. Scanning electron micrographs of a: (0003), gibbsite; b: (0004), boehmite; c: (0010), wet ground gibbsite (110 h); d: (0002), dry ground boehmite (350 h).

against rehydration. The one-pulse spectra were obtained at 130.3 MHz with the following settings: pulse width was 1.25 μs, the size was 4096 data points, and the sweep width was $\pm$20 kHz. The number of accumulations was typically 3–5 $\times$ 10^3. The 90° pulse width for the reference 0.1 *M* $AlCl_3$ solution was ~5 μs. According to Lippmaa *et al.* (*3*, Eq. 1) the pulse width for a selective excitation of the centerband in a solid should be about one-tenth of the solution 90° pulse width for a nucleus with $I = \frac{5}{2}$. ^{27}Al MAS NMR spectra have been recorded with pulse lengths between 0.5 and 2 μs. It was found that relative to the intensity of the Al^{VI} line, the intensity of the Al^{IV} and Al^{V} lines decreased by about 10% between the two extremes, the strongest intensity for both these lines being obtained with the 0.5-μs pulse width. With a 1.25-μs pulse width the decrease in relative intensity was less than 5%, while the absolute intensity of the overall signal was larger. If we consider how the relative intensity of the $-\frac{1}{2}$ to $\frac{1}{2}$ central transition changes with pulse length and ν_Q, as shown in Fig. II.36 of Engelhardt and Michel's book (*22*) (ν_1 = 42 kHz), the intensity reaches a maximum for a pulse width between 2 and 2.5 μs for $\nu_Q > 500$ kHz (or QCC > 3.3 MHz). As shown later in our experiment ν_1 is about 1.7 times larger and a pulse width of 1.2 μs seems to be an adequate compromise for selective irradiation and overall intensity of the center transition of nuclei with QCC in excess of 3 MHz.

The spinning rate was between 9 and 11 kHz. On one selected sample, in which the ~30-ppm line assigned to Al^{V} was intense,

one-pulse spectra were recorded at 104.2 and 78.2 MHz. On the same sample, a two-dimensional (2D) nutation experiment was performed, as defined by Samoson *et al.* (*6,26*) and Kentgens *et al.* (*25*). The spectra were acquired with a radio frequency ($\Omega_{rf}/2\pi$) of 73 kHz. Two hundred fifty-six spectra were recorded with pulse width increments of 1.5 μs. The pulse width ranged from 0.5 to 384 μs and 1000 accumulations were made for each spectrum.

The carrier frequency was set at the center of the Al spectrum, that is, at ~30 ppm, and the delay time was 50 ms. Each row along the so-called F_2 axis, or chemical shift axis, contained 2048 data points in the real space. To each point along F_2 was associated a column along the quadrupole interaction axis F_1 and each column contained 256 data points, corresponding to the 256 spectra. The free induction decay was Fourier transformed (FT) and the corresponding spectra obtained were converted to magnitude spectra. These spectra were stored along the F_2 axis. These same operations were repeated for each column (along F_1). The final result of this operation is a 2D representation (F_2, F_1) displaying the quadrupole interaction F_1 and the chemical shift F_2. A variant of this procedure is in applying a "sine bell" apodization along F_1 and F_2 before FT.

The significant unit along F_1 is the strength of the rf magnetic field (H_1), which is expressed as its frequency by the following equation: $\nu_1 = \Omega_{rf}/2\pi = \gamma_{Al/2\pi}H_1$. In our experimentation the rf power was 170 W. The value of $\Omega_{rf}/2\pi$ was calculated from a nutation spectrum of ^{23}Na in NaCl (whose quadrupole coupling constant QCC = 0). This lengthy technique yields the actual Ω_{rf}. When the Ω_{rf} value is approximated by determining the 90° pulse width, which gives the maximum intensity of the ^{27}Al peak of a 0.1 *M* $AlCl_3$ solution, there is considerable experimental error due to appreciable differences in the Q factor of the resonating circuit.

EPR measurement. Alumina samples were purified in a flow of O_2 at 550–600°C to remove organic contaminants. It should be noted that aluminas ex-ground boehmite were highly contaminated by carbonaceous residue as witnessed by an EPR signal at g = 2.003 and a peak-to-peak linewidth of about 6 G. ^{27}Al MAS NMR spectra were also recorded after the oxidation treatment to check the eventual transformation of the samples. As shown later, this is a useful precaution. After oxidation the samples were carefully outgassed for several hours at 550–600°C. *N,N*-Dimethylaniline, previously purified with the freeze–thaw method, was condensed from the saturated vapor on the alumina by cooling the EPR tube for a short time. EPR spectra were recorded after contact times between 1 and 48 h. Generally, a contact time as long as 20 h was necessary to obtain relatively intense spectra. The EPR spectra were recorded at room temperature on a Varian E-115 spectrometer using the X band. The settings are indicated in the figure captions. Afterward O_2 is introduced into the EPR tube and the spectrum is recorded again before and after outgassing for 1 h at room temperature.

RESULTS

The ^{27}Al MAS spectra of the gibbsite and boehmite precursors are characterized by one single line corresponding to sixfold-coordinated aluminum. The center of gravity or the chemical shift (δ_{CG}) of this line is at 8.5 ppm in boehmite and 8.8 ppm in gibbsite. The reproducibility is within ±0.2 ppm for the Al^{VI} resonance. The full width at half-height ($\nu_{1/2}$) is in both cases 6.5 ± 0.5 ppm. The only difference between the two precursors is in the presence of a weak shoulder on the upfield side of the Al^{VI} resonance in gibbsite. Dry ground gibbsite has a very weak line at ~61.0 ppm and somewhat stronger line at 34 ppm, in addition to the Al^{VI} line at 9 ppm. The $\nu_{1/2}$ of the latter is 8 ppm. Wet ground gibbsite has a similar spectrum, except that at ~30 ppm a weak shoulder instead of a peak is observed.

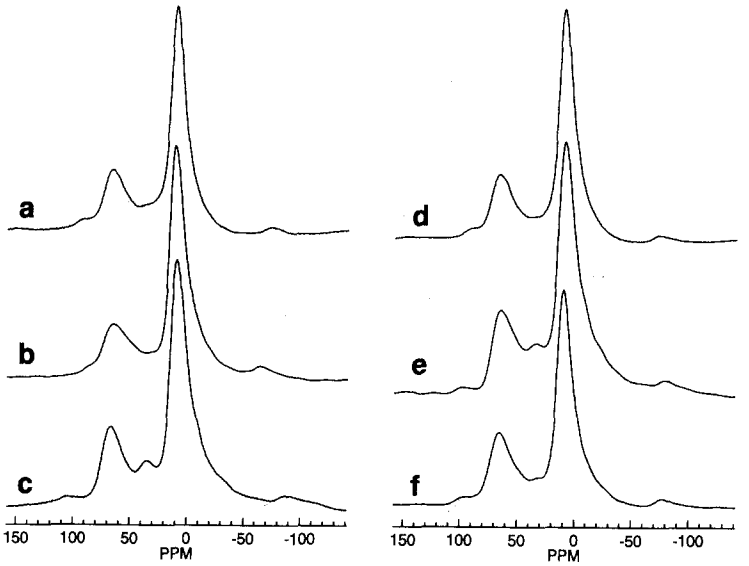

FIG. 2. One-pulse ^{27}Al MAS spectra. Spinning rate between 10 and 12 kHz. (a) Gibbsite calcined at 400°C (1 h); (b) wet ground gibbsite (110 h) calcined at 400°C (1 h); (c) dry ground gibbsite (125 h) calcined at 500°C (1 h); (d) gibbsite calcined 500°C (1 h); (e) dry ground gibbsite (125 h) calcined at 600°C (1 h); (f) e calcined one additional hour at 800°C. The spinning side bands are outside the range of chemical shifts of the three Al resonances.

Upon dehydroxylation the spectra become more complicated and a clear cut is observed between the aluminas ex-gibbsite or wet ground gibbsite on the one hand, and ex-dry ground gibbsite on the other hand. This is shown by selected examples in Fig. 2. At 400°C and up to 700°C, the ^{27}Al MAS spectra of aluminas ex-gibbsite or wet ground gibbsite contain two broad lines: one with δ_{CG} between 65 and 66 ppm attributable to Al^{IV} and a second one with δ_{CG} between 9.5 and 11 ppm due to Al^{VI}. The aluminas ex-dry ground gibbsite contain, in addition, the line with δ_{CG} at about 35 ppm upon calcination at 400°C. This line is still detectable at 500°C, but it weakens at 600°C (not shown) and it becomes hardly detectable at 700°C. At 800°C it vanished. Qualitatively these observations are in good agreement with those reported by Paramzin *et al.* (*17*).

The effects of dehydroxylation on unground and ground boehmite are more spectacular, as shown in Fig. 3 and Fig. 4. Figure 3a shows that dehydroxylation and subsequent formation of alumina do not occur in boehmite heated at 400°C, in agreement with the observation that the endothermic loss of constitutional water occurs at 450°C. Uncalcined ground boehmite (Fig. 3b) has an ^{27}Al spectrum which contains about 28 and 16% of the overall intensity in the lines at 34 and 63 ppm, respectively. The Al^{VI} line is broadened as a result of the amorphization of the material. Upon calcination at 400°C the width of the Al^{VI} line increases again and the 63-ppm line contains ~26% of the total intensity, whereas the intensity of the 34-ppm line remains unchanged (Fig. 3c). The apparent increase in intensity of this line with respect to that in spectrum b in Fig. 3b is due to the broadening of the Al^{VI} line and the increase in intensity of the Al^{IV} line (at 63 ppm). After calcination for 3 h at 600°C the alumina ex-boehmite and the alumina ex-ground boehmite have very different ^{27}Al MAS spectra. The former contains two main lines at 66 ppm (Al^{IV}) and at ~10 ppm. Spectrum d in Fig. 3 is, thus, very similar to that

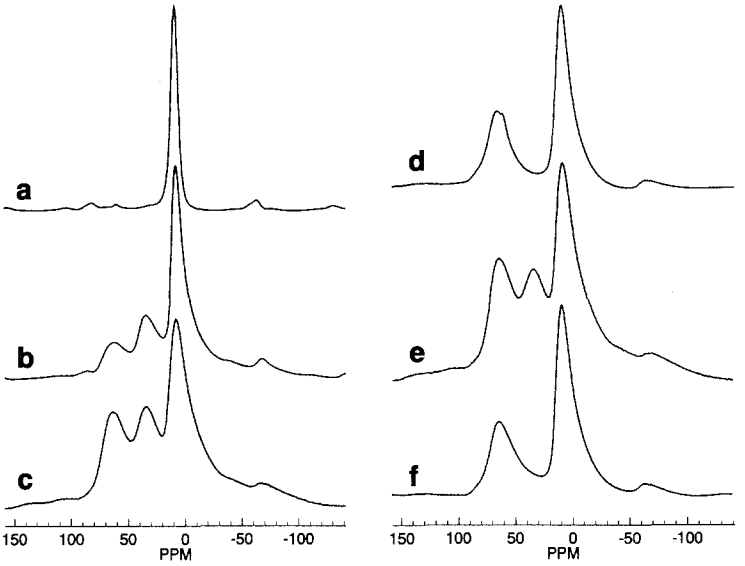

FIG. 3. One-pulse ^{27}Al MAS spectra: (a) boehmite heated at 400°C (1 h); (b) uncalcined ground boehmite; (c) ground boehmite (350 h) heated at 400°C (1 h); (d) boehmite heated at 600°C for 1 h; (e) ground boehmite calcined at 600°C, 1 h; (f) e heated at 800°C for 1 h. The spinning rate is between 9.5 and 9.8 kHz.

observed for ex-gibbsite aluminas, but for the small splitting of the line at 66 ppm. The alumina ex-ground boehmite (Fig. 3e) has the strong additional line at 34 ppm. This line is much stronger than that observed for the alumina ex-dry ground gibbsite (Fig. 2e). When the dehydroxylation temperature is 800°C (1 h calcination) alumina ex-ground

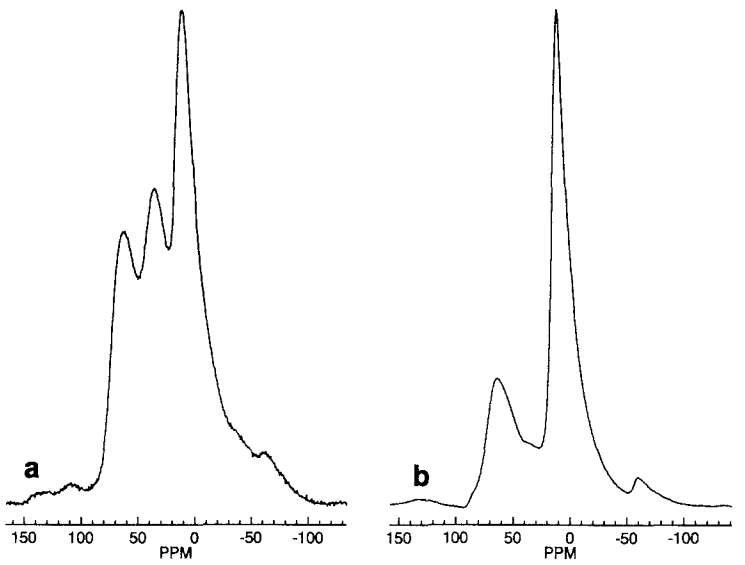

FIG. 4. Comparison of the thermal stability of the aluminas: (a) ex-ground boehmite (350 h) calcined in O_2 for 6 days at 550°C; (b) ex-ground gibbsite (125 h) calcined 1 h at 400°C and 1 h at 600°C in O_2.

boehmite (Fig. 3f) exhibits the same ^{27}Al spectrum as the alumina ex-boehmite or ex-gibbsite (Fig. 2d). There is no longer a line at 34 ppm. Already at 700°C this line becomes hardly observable. Thus, above ~700°C the aluminas ex-ground or unground boehmite or gibbsite have a similar "structure."

The Al^V coordination assigned to the line at 34 ppm is more thermally stable in ground boehmite than in dry ground gibbsite. This is shown in Figs. 4a and b. Figure 4a shows the ^{27}Al spectrum of the alumina ex-ground boehmite treated for 6 days at 550°C in a flow of oxygen, whereas Fig. 4b shows the spectrum of an alumina ex-ground gibbsite first calcined for 1 h at 400°C, at which stage the spectrum in Fig. 2c is obtained, and then calcined for 1 h at 600°C. Obviously, the structure of the alumina ex-ground boehmite is more stable. On a more quantitative basis the aluminas without the 34-ppm line have about a 2/1 Al^{VI}/Al^{IV} ratio. The aluminas obtained ex-ground boehmite and calcined between 500 and 600°C have the composition $Al^{VI} = 45\%$, $Al^{IV} \simeq Al^V = 27.5\%$, whereas the aluminas ex-ground gibbsite have the composition $Al^{VI} = 60\%$, $Al^V = 10\%$, $Al^{IV} = 30\%$ for calcination temperature between 400 and 500°C. Above 600°C their Al^V content decreases to about 6% at 600°C and it is below 3% at 700°C. Due to the width and to the overlapping of the lines, the accuracy of these deconvolutions is not very satisfactory. From repeated deconvolutions of spectra recorded for identical samples it comes out that the *relative* error on the integrated area of a line with intensity ≥25% is about ±10%, while it can reach ±20% on a line with integrated area ~10%. The overall absolute intensity of the ^{27}Al NMR spectra does not change with the preparation procedure and, in particular, with the variation in the surface area reported in Table 1. Under our experimental conditions there is apparently no systematic change attributable to a factor other than the loading of the spinner on the line intensity. For instance, consider in Table 2 the absolute intensity of the ^{27}Al signals in ex-boehmite aluminas referred to the intensity obtained for the nonheated sample. The observed variations are small and independent of the surface area in spite of the tremendous change observed in the shape of the spectra shown in Fig. 3.

TABLE 2

Comparison of the Absolute Intensity of the ^{27}Al Signal of Ex-boehmite Aluminas with Respect to the Thermal Treatment and Surface Areas, the Untreated Sample Being the Reference

Sample	Temperature (°C)	Surface (m^2/g)	Absolute intensity/reference
Unground boehmite	RT	9	1
	400	9	1.16
	600	70	1.08
Ground boehmite	RT	130	1
	400	126	0.96
	500	110	1.2
	600	104	0.98

Whatever the nature of the aluminas, the observed chemical shifts (δ_{CG}) at the peak maxima are spread over a narrow frequency range. In all cases, Al^{VI} is observed at 8 ± 1 ppm. Al^{IV} is at 64 ± 1 ppm and Al^V is at 34 ± 1 ppm. Since the isotropic chemical shifts δ_{CS} are related to δ_{CG} by the equation

$$\delta_{CG} = \delta_{CS} + \delta_{QS} \quad (1)$$

and the second-order quadrupolar correction on the central transition is (*3*)

$$\delta_{QS}\,(\text{ppm}) = -6 \times 10^3 \left[\frac{QCC}{\nu_L}\right]^2 (1 + \eta^2/3) \quad (2)$$

the correction depends upon the magnitude of the quadrupole coupling constant [QCC in Eq. (2)], the Larmor frequency ν_L, and the asymmetry of the electric field gradient at the nucleus η. From the lineshape it may be assumed that η is close to 1. QCC is not known. One way to obtain QCC is to record spectra for the same sample at different fields. Indeed, δ_{CG} must be a linear function of ν_L^{-2} and the slope gives $(QCC)^2(1 + \eta^2/3)$. The other technique mentioned in the Introduction and explained under Techniques: ^{27}Al NMR Resonance is in recording nutation spectra. Both techniques have

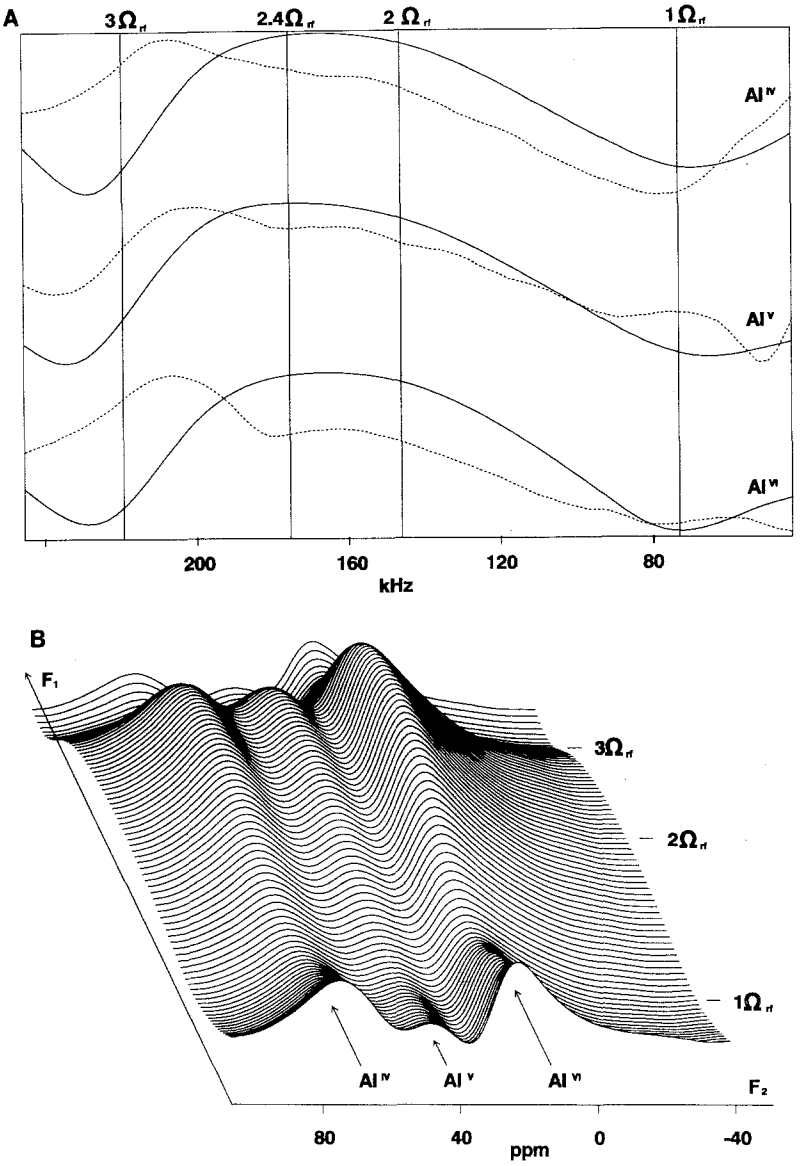

FIG. 5. (A) Projections of the quadrupole spectra on the quadrupole interaction axis corresponding to the peak maxima at the Al^{IV}, Al^{V}, and Al^{VI} resonances. $n\Omega_{rf}$ are indicated as references. (B) Two-dimensional representation of the nutation experiment F_1, quadrupolar interaction; F_2, chemical shift axis.

been applied to an alumina ex-ground boehmite in which the proportions of Al^{V} and Al^{IV} are almost equal (see Fig. 3c). The results of the nutation experiment are displayed in Figs. 5A and B. In Fig. 5A, the quadrupole spectra along F_1 are shown for the Al^{IV}, Al^{V}, and Al^{IV} resonances, without (solid line) and with (dashed line) sine bell apodization (*23*). These spectra are broad and featureless, although a somewhat better resolution is achieved with sine bell apodization.

Figure 5B shows the 2D nutation experiment as a stacked plot of spectra along F_1,

the first spectrum being at 34 kHz and the last one at 243 kHz along this axis (no sine bell apodization was applied for this representation). The intensity modulations along F_1 have to be compared with the quadrupole spectra shown by the solid lines in Fig. 5A. A clear cut is observed as $3.\Omega_{rf}$ is approached.

When a nutation experiment is performed on a NaY zeolite using identical conditions, the nutation spectrum along the F_1 dimension, corresponding to the resonance at 60 ppm Al^{VI}, contains one peak centered on $1.\Omega_{rf}$ and extending from about 40 to 100 kHz. This peak is followed by weak modulations and preceded by a noticeable increase in intensity as $F_1 = 0$ is approached. It is similar to that shown in Fig. 2 of Ref. (*6*). The comparison of calculated and experimental nutation spectra by Samoson and Lippma (*24*) yields a QCC of 2 MHz for Al^{IV} in NaY.

The origin of anomalous high intensity near $F_1 = 0$ has been discussed by Kentgens *et al.* (*25*) who showed that it is due to an off-resonance term in the secular Hamiltonian in the rotating frame. The lowest intensity in this region is obtained by irradiating at the Larmor resonance. In the case of a sample containing ^{27}Al in three different coordinations and, thus, three resonance frequencies, irradiating near the center of the resonance spectrum near 30 ppm is the only possible solution. This way introduces, of course, offset terms. Because of the broadness of the nutation spectra shown in Fig. 5A, only an estimate of the range over which the QCCs are distributed is possible. Kentgens *et al.* (*25*) have calculated for spin $I = \frac{5}{2}$ nutation spectra for a large range of Ω_Q/Ω_{rf}. At low QCC the main feature is a peak at $1.\Omega_{rf}$ as observed in NaY. As Ω_Q/Ω_{rf} increases, this feature decreases in relative intensity whereas a new feature appears between $1.\Omega_{rf}$ and $3.\Omega_{rf}$. The intensity of this new feature increases and it shifts toward $3.\Omega_{rf}$ with increasing QCC. As a result and as shown in Fig. 7 of Ref. (*26*), the center of gravity of the nutation spectrum shifts toward $3.\Omega_{rf}$ as QCC increases. With a center of gravity near $2.4\Omega_{rf}$ as observed in Fig. 5A the QCC should be at least 4 to 5 MHz, but to what extent one can define an "average" QCC from the center of gravity is questionable.

Therefore, the information contained in the nutation spectra of Fig. 5A is limited, but nevertheless important: (i) all three kinds of aluminum nuclei, namely Al^{IV}, Al^{V}, and Al^{VI}, have the same distribution of QCCs and similar "average QCCs," and (ii) the three kinds of coordination polyhedra have similar distortion.

Recording the resonance spectra at three different Larmor frequencies permits one to measure the variation of δ_{CG} and, thus, an average QCC (Table 3). For the three resonances a QCC near 2.5 MHz fits Eqs. (1) and (2) resonably well. Such a low value of QCC is surprising, if compared with the

TABLE 3

Average Isotropic Chemical Shift (δ_{CS}) Calculated from Eq. (2) and Using QCC = 2.5 MHz, δ_{CG} Calculated [Eq. (1,2)], and δ_{CG} Observed

	δ_{CS} (ppm)	ν_L = 130.3 MHz		ν_L = 104.2 MHz		ν_L = 78.2 MHz	
		δ_{CG}(calc) (ppm)	δ_{CG}(obs) (ppm)	δ_{CG}(calc) (ppm)	δ_{CG}(obs) (ppm)	δ_{CG}(calc) (ppm)	δ_{CG}(obs) (ppm)
Al^{VI}	11.4 ± 0.3	8.5	9	6.8	6.5	3.2	4 ± 1
Al^{V}	38.3 ± 1.3	35.4	34.1	33.7	35.1	—	—
Al^{IV}	65.6 ± 0.2	62.7	62.5	61	61.2	57.4	(60.8)

large distribution of QCCs revealed by the nutation spectra and the corresponding "average QCCs" derived from them.

In conclusion to the "structural" part of this study, it is clear that the main difference between the thermally activated ex-boehmite and ex-gibbsite aluminas is the relative amount of Al^{V}. The ratio Al^{IV}/Al^{VI} remains roughly constant and the degree of distortion of the Al^{VI}, Al^{V}, and Al^{IV} polyhedra spreads over a similar broad range. Another interesting point is that Al^{V} coordination is thermally unstable.

The historical conception for a Lewis acid site, as a site able to accept a lone pair of electrons from a Lewis base, would require threefold-coordinated aluminum, Al^{III}. There is no evidence that NMR would detect trigonal alumina either because the QCC of this species would be huge or because its concentration would be too small. In fact, considering the energy of an Al–O bond, Al^{III} should convert to a higher coordination when exposed to traces of water vapor and/or of oxygen. The existence of Al^{III} in practical catalysis, therefore, seems doubtful.

The Lewis concept of acidity goes back to the distinction between covalent and ionic bonding: so many examples of partially covalent–ionic bonds supply a more general definition of a Lewis site as an electron acceptor site. In the presence of Lewis base there would be an increase in electron density within the Al coordination polyhedron. Of course, any distorted polyhedron with oxygen vacancy would favor such a transferred electron density. The metastability of Al^{V} coordination shells near the surface may play an important role since this state of coordination easily transforms into either Al^{IV} or Al^{VI}, which means that of two Al^{V} shells one has to lose an oxygen. The transient state in this transformation might create the favorable configuration for an electron-deficient site. The problem is that the number of active Lewis sites on a surface may be smaller by a factor of 100 than the number of surface sites, bringing about 10^{18} active sites per gram for an alumina with a surface area of 100 m^2/g. Therefore, an alumina in which Al^{V} is not detected by MAS NMR could still have enough of the active sites linked to or generated by this configuration, which could be detected by a sensitive surface technique. Of course, the probability of having these sites is likely to be higher when a large number of Al^{V} is observed.

EPR Results

As outlined in the Introduction aniline failed to give EPR signals when chemisorbed on the aluminas studied here. Dimethylaniline (DMA) (ionization potential: 7.1 eV) has produced a consistent EPR signal which can be assigned, by analogy with the information obtained for aniline (*19*), to a radical cation.

This signal is shown in Figs. 6a and b. It

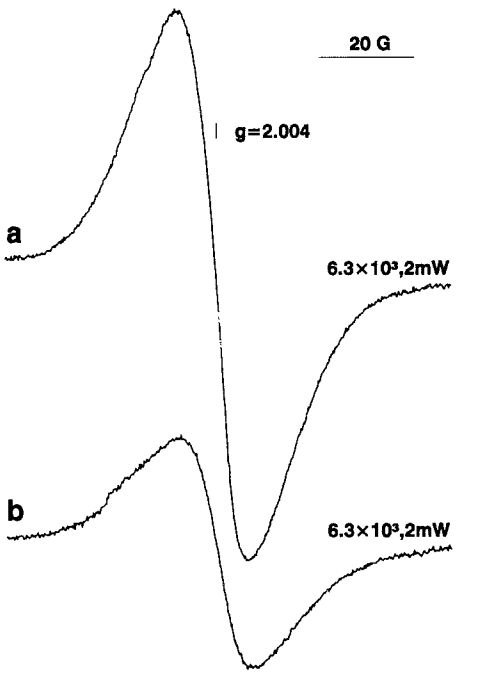

FIG. 6. EPR spectra obtained at RT for *N,N'*-dimethylaniline chemisorbed (a) on ground boehmite heated at 550°C for 6 days (see the ^{27}Al spectrum a in Fig. 4) and (b) on boehmite heated at 600°C for 1 h (see the ^{27}Al spectrum d in Fig. 3). The integrated intensity of spectra a and b are 3.8×10^{17} and 1.6×10^{17} spins g^{-1}, respectively. The contact time was 48 h in both cases.

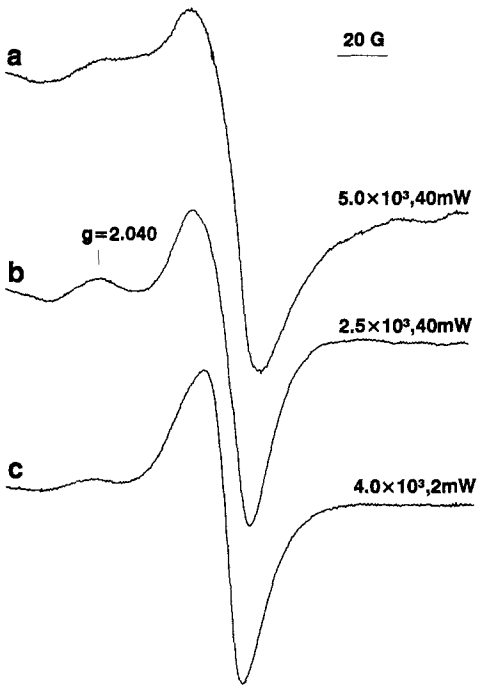

FIG. 7. EPR spectra obtained at RT after adsorption of *N,N'*-dimethylaniline and exposure to O_2 of (a) sample A in Fig. 5; (b) after outgassing O_2 for 1 h at RT; (c) the same as in b at lower power.

is featureless and the integrated intensity (obtained from the second integral) in (a) is more than twice the intensity in (b). The alumina ex-ground boehmite (spectrum c in Fig. 3) is rich in Al^V, whereas that used for (b) (spectrum d in Fig. 3) does not contain detectable Al^V.

Upon adsorption of O_2 (PO_2 = 200 Torr), after exposure to DMA, the spectrum shown in Fig. 6a is modified into spectrum a in Fig. 7 and, after evacuation of O_2, into spectrum b in Fig. 7. Spectrum 7b is very similar to that observed on γ-Al_2O_3 treated by N_2O and assigned by Losee (*21*) to O_2^-. No hyperfine structure is observed, in contrast with the situation described for O_2 adsorbed on aniline-treated dealuminated H-mordenite where six lines with a splitting of 5–6 G were recorded (*19*). Thus, there is no direct proof that O_2 interacts with the Al nucleus ($I = \frac{5}{2}$) in aluminas. However, the g_{zz} value is about the same as that reported for O_2 interacting with aluminum in zeolite (*19*). Spectrum b in Fig. 7 could be simulated with a g_{zz} hyperfine splitting smaller than 5 G and a linewidth on the order of 10 G. The intensity of the EPR spectrum 7b is about three times larger than the intensity of spectrum 6a which, itself, is about two times larger than 6b.

Upon exposure to O_2, spectrum 6b undergoes the same change as spectrum 6a, but the intensity is three times smaller. The difference between spectra 6a and 6b must be related to the difference in the surface composition of the two aluminas. If O_2^- is stabilized by interaction with a Lewis site linked to aluminum, the main difference between aluminas containing an appreciable amount of Al^V (Fig. 6a) or without detectable Al^V (Fig. 6b) is either in the number of Lewis sites, of equal strength, or in the distributions of the Lewis sites with respect to their strengths. We insist again that no signal attributable to O_2^- is detectable in the absence of preadsorbed DMA.

Since the difference in the ionization potentials of aniline and DMA is 0.6 eV, the electron affinity of the Lewis sites in dealuminated zeolite is lower by −0.6 eV than that of the Lewis sites in transition aluminas. This difference in Lewis acid strength could also be responsible for a smaller hyperfine splitting in O_2^- adsorbed on alumina, as compared to that observed for O_2^- in dealuminated zeolites, since the hyperfine splitting is proportional to the electron density on the site.

We summarize the EPR results as follows. On transition aluminas, dimethylaniline forms a radical cation by sharing an electron with electron-deficient sites ($R \rightarrow L^- + R^{+\cdot}$). Upon further exposure to O_2 the electron of L^- is transferrred to LO_2^- and L is probably a site related to aluminum. Aluminas containing Al^V have more electron-deficient sites than aluminas containing solely Al^{IV} and Al^{VI}.

DISCUSSION

Since this work aims to study to what extent structural defects contribute to the acid character of an alumina surface, it is

appropriate, in the first approximation where distortion is not taken into account, to examine the influence on the local charge brought by oxygen atoms of the distribution of aluminum over different coordination shells. This can be achieved for a spinel structure with composition $Al_{21.33}O_{32}$ where, out of 24 cationic sites, a fraction $X_D = 0.111$ are vacant and where the fractional X_D (octahedral Al^{VI}) and X_T (tetrahedral Al^{IV}) are 0.592 and 0.296, respectively (*4,5*).

In such an idealized spinel structure, each oxygen is common to three octahedra and one tetrahedron. Because of the cationic vacancies three kinds of oxygen can be distinguished, namely, O_a bound to three Al^{VI} and one Al^{IV}, O_b bound to three Al^{VI} and a vacancy, and O_c bound to two Al^{VI}, one Al^{IV}, and one vacancy. If X_O, X_T, and X_D are the probabilities for a cationic site to be occupied by Al^{VI}, Al^{IV}, and a vacancy, respectively, the following equation must be fulfilled:

$$X_O + X_T + X_D = 1 = 0.5923 + 0.2963 + 0.1111. \quad (3)$$

In such a spinel the Al^{VI}/Al^{IV} ratio is 2, as expected (*5*), and in agreement with the experimental ratio obtained in this study. N being a normalization factor, the number of O_a is $NX_O{}^3X_T$, the number of O_b is $NX_O{}^3X_D$, whereas the number of O_c is $NX_O{}^2X_TX_D$ if the sites are randomly distributed and

$$N[X_O{}^3X_T + X_O{}^3X_D + X_O{}^2X_TX_D] = 32. \quad (4)$$

From Eq. (4) the numbers of O_a, O_b, and O_c are 20.47, 7.6777, and 3.84, respectively. The electrostatic bond strengths (EBSs) with Pauling's definition of O_a, O_b, and O_c are 2.25, 1.5, and 1.75, respectively. If this way of reasoning is correct, the electroneutrality condition should be

$$N[2.25X_O{}^3X_T + 1.5X_O{}^3X_D + 1.75X_O{}^2X_TX_D] = 64 \quad (5)$$

or from (4) and (5),

$$R = \frac{2.25X_O{}^3X_T + 1.5X_O{}^3X_D + 1.75X_O{}^2X_TX_D}{X_O{}^3X_T + X_O{}^3X_D + X_O{}^2X_TX_D} = 2.$$

The experimental values of R calculated from the NMR X_O and X_T in aluminas, without Al^V, are 2 ± 5%.

Now consider an alumina containing Al^{VI}, Al^V, and Al^{IV} and assume that the chemical formula $Al_{21.33}O_{32}$ remains unchanged. There are now six kinds of oxygen O_a . . . O_f with the following arrangements, *a priori* probabilities, and EBSs:

	O_a	O_b	O_c	O_d	O_e	O_f
	$X_O{}^3X_D$	$X_O{}^3X_T$	$X_O{}^2X_PX_D$	$X_OX_PX_TX_D$	$X_P{}^2X_TX_D$	$X_O{}^2X_TX_D$
EBS	1.5	2.25	1.6	1.85	1.95	1.75

X_p is the fraction of pentacoordinated Al^V. If we use the alumina in which X_O, X_T, and X_P are in the ratio 2 : 1 : 1, namely that obtained for the ex-ground boehmite alumina calcined at 500°C, X_D being unchanged, it follows that

$$X_O = 0.444, \quad X_T = X_P = 0.2222, \quad \text{and } X_D = 0.1111.$$

The suggested coordinations of oxygen to aluminum are founded on the structure of andalusite (*1*) and on the assumption that each oxygen is still common to four sites. In andalusite where Al^V is in a square pyramid, one oxygen can be coordinated to two Al^V and one tetrahedral site (occupied by silicon), but oxygen cannot be common to two tetrahedral sites. Using the above values of X one finds $N_a = 7.134$, $N_b = 14.628$, $N_c = N_f = 3.657$, $N_d = 1.829$, and $N_e = 0.9144$, and R is 1.92, thus, still within acceptable limits. The diagram in Fig. 8 represents the

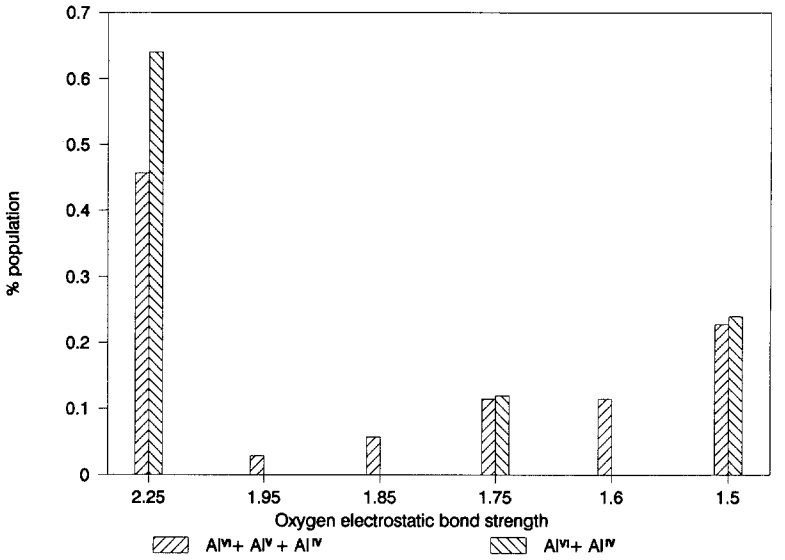

FIG. 8. Bulk distribution of the oxygen atoms population with respect to their electrostatic bond strengths (EBS) in two extreme models, namely, an ideal pseudospinel containing Al^{VI} and Al^{IV} only and in the transition alumina containing 50% Al^{VI}, 25% Al^{IV}, and 25% Al^{V}.

distribution of the oxygen atom population with respect to their electrostatic bond strength for spinels with or without Al^{V}. We observe that 35% of the oxygens in an alumina with the Al^{VI}/Al^{IV} expected for a spinel without Al^{V} have an EBS < 2, whereas in an alumina with the indicated proportions of Al^{VI}, Al^{V}, and Al^{IV}, 55% of the oxygens have an EBS < 2. Thus, in an idealized Al spinel network, the presence of Al^{V} increases the relative proportion of oxygen atoms with nominal charge < 2.

On a terminal lattice plane at the surface of a crystallite, the dangling bonds are replaced by surface OH. In hydrated γ-Al_2O_3, the ^{17}O resonance experiments by Walter and Oldfield (*27*) revealed two resonance lines: one shifted by 70 ppm and the other shifted by 50 ppm with respect to H_2O. Surface OH contributes partially to the latter, as revealed by proton cross-polarization. Nonhydroxylic oxygens contribute to the 70-ppm line (QCC $\simeq$ 2 MHz) and partially to the 50-ppm line (QCC $\geq$ 4 MHz). Again, in postulating that the surface composition is qualitatively, but not quantitatively, similar to the bulk composition, the possible existence of at least two kinds of nonhydroxylated surface oxygens would be in agreement with the presence of O_a, O_b, and O_c [as in Eq. (4)] in an alumina without Al^{V}. The thermal activation needed to achieve catalytic activity in removing surface hydroxyls restructured the surface. On the basis of infrared studies, Knözinger and Ratnasamy (*28*) suggested assignments of surface hydroxyl stretching frequencies with respect to the EBS of surface oxygens and they showed that dehydroxylation is not a random process: depending upon their EBS, some sites are privileged for nucleating water molecules.

In the restructuring process, the lability of the structural elements must play an important role, ruling the final, active configuration. Since Al^{V} is mestastable, even in the bulk, it should *a priori* be important in determining the distribution of active sites on the surface. This circumstantial evidence supports the idea that a surface, originally rich in Al^{V}, contains, after restructuring, more electron acceptor sites (here consid-

ered as active Lewis sites), because it is more likely to have aluminum with strongly perturbed oxygen coordination than a surface originally poor in Al^V.

It has been shown in the present study that thermal treatment beyond 600°C rapidly decreases the number of Al^V sites. Labile sites can indeed be suspected to generate surface configurations which would be less probable otherwise. As a matter of fact, we have reported that the number of sites able to abstract an electron from dimethylaniline was about double in aluminas containing a relatively large number of Al^V, as compared with those without detectable Al^V. In the former case the number of spins was about 4×10^{17} g, which means that on a surface area of 100 $m^2 g^{-1}$ there are 4.10^{11} sites/cm^2 able to ionize DMA, that is, sites with an electron affinity larger than than $|-7.1$ eV$|$. On aluminas without NMR-detectable Al^V, this number is smaller by a factor of ~2.

From a straightforward calculation of oxygen vacancies resulting from the dehydroxylation of the 111 face of a transition alumina, Knözinger and Ratnasamy (*28*) found a number of surface sites in the range of 10^{14} sites/cm^2, but they also report that the number of strongly bound CO on γ-Al_2O_3 is about 6×10^{12}/cm^2. These figures are about 10 times larger than those obtained for the demanding formation of the dimethylaniline radical cation and about 10 times lower than the number of calculated oxygen vacancies. This shows that the description of Hall and co-workers (*29,30*) of active sites (on aluminas) as "special exposed aluminum cations" is fundamentally correct even though the "real" exposure may actually result from a "distorted coordination." Here, we do not claim that a special kind of Al is directly responsible for the existence of Lewis sites. We state that indirect evidence suggests that, due to its metastability and its influence on the formal charge of neighboring oxygens, Al^V is more likely to generate these sites.

As far as the Lewis activity is concerned, the fact that small-sized dehydroxylated boehmite is much richer in Al^V than its larger particle sized counterpart is interesting for understanding not only the behavior of aluminas, but that of dealuminated zeolites as well. Indeed, it has been suggested by Shannon *et al.* (*31*) that the alumina precursor in dealuminated zeolite has a boehmite structure. Because this precursor is likely to be dispersed within the zeolite cages in very small slabs, it is not surprising that signals corresponding to Al^V are found in dealuminated or steamed H zeolites. Moreover, since in some way the presence of Al^V is linked to a relatively large number of strong Lewis sites, the presence of the Al^V signal (at ~30 ppm) in such samples is meaningful. In Fig. 9 are shown simulated ^{27}Al MAS

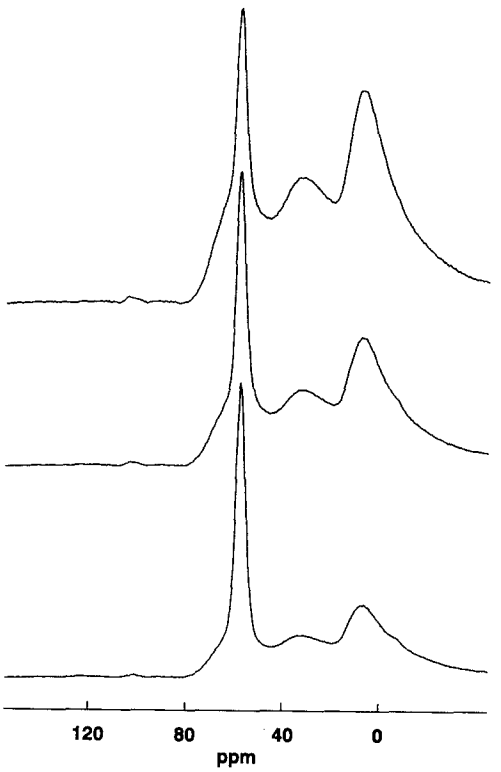

FIG. 9. Simulated ^{27}Al MAS NMR spectra obtained by "mixing" the experimental spectrum obtained for NaY zeolite with the experimental spectrum obtained for a ground boehmite heated at 600°C for 1 h (spectrum e in Fig. 3). From top to bottom mixing is 1/2. 1/1, and 1/0.5, the second figure being the multiplication factor applied to the spectrum of the alumina phase. These simulated spectra could be compared, for instance, to those shown in Fig. 2 of Ref. (*9*) obtained for steamed HY zeolites.

spectra obtained by "mixing" the ^{27}Al spectrum of NaY with the ^{27}Al spectrum shown in Fig. 3d. These mixed spectra are, indeed, very similar to those reported in the references mentioned in the Introduction. As recalled earlier aniline yields radical cation on dealuminated H-zeolites and not on aluminas. The lower electron affinity of the Lewis sites in aluminas with respect to those in dealuminated H-zeolites *might* indicate a synergistic effect between the nonframework aluminum site and the nearby proton of a strong Brønsted acid site in zeolite.

ACKNOWLEDGMENTS

This work is supported by DOE Grant DE-FG02-90 ER1430. One of us (F. R. Chen) thanks Unocal (California) for financial support. NSF Grant DIR-8719808 and NIH Grant RR 04095, which have partly supported the purchase of the GN 500 NMR instrument, are also gratefully acknowledged.

We would also like to thank Dr. G. J. Ray (AMOCO) and Professor B. Gerstein (Ames, Iowa) for recording ^{27}Al mass spectra at lower frequencies (Table 3).

REFERENCES

1. Burnham, C. W., and Buerger, M. J., *Z. Kristallogr.* **115,** 269 (1961)
2. Alemany, L. B., and Kirker, G. W., *J. Am. Chem. Soc.* **108,** 6158 (1986).
3. Lippmaa, E., Samoson, A., and Mägi, *J. Am. Chem. Soc.* **108,** 1730 (1986).
4. Bragg, W. S., "Atomic Structure of Minerals." Cornell Univ. Press, Ithaca, NY, 1937.
5. Wells, A. F., "Structural Inorganic Chemistry," 3rd ed. (1962), Oxford Univ. Press (Clarendon), London.
6. Samoson, A., Lippmaa, E., Engelhardt, G., Lohse, U., and Jerschewitz, H. G., *Chem. Phys. Lett.* **134,** 589 (1987).
7. Pellet, R. J., Scott-Blackwell, C., and Rabo, J. A., *J. Catal.* **114,** 71 (1988).
8. Man, R. P., and Klinowsky, J., *Chem. Phys. Lett.* **147,** 581 (1988).
9. Sanz, J., Fornes, V., and Corma A., *J. Chem. Soc. Faraday Trans. 1* **84** (9), 3113 (1988).
10. Ray, G. J., Meyers, B. L., and Marshall, C. L., *Zeolites* **7,** 307 (1987).
11. Grobet, P. J., Geerts, H., Martens, J., and Jacobs, P. A., *J. Chem. Soc. Chem. Commun.*, 1688 (1987).
12. Gilson, J. P., Edwards, G. C., Peters, A. W., Rajagopalan, K., Wormsbecker, R. F., Roberie, T. G., and Shatlock, M. P., *J. Chem. Soc. Chem. Commun.*, 91, (1987).
13. Lambert, J. F., Millmann, W. S., and Fripiat, J. J., *J. Am. Chem. Soc.* **111,** 3517 (1989).
14. Deng, Z., Lambert, J. F., and Fripiat, J. J., *Chem. Mat.* **1,** 640 (1989).
15. Dupree, R,. Farnan, I., Forty, A. J., El-Mashri, S., and Bottyan, L., *J. Phys. Colloq. 68* **46,** 113 (1985).
16. Oka, Y., Takahashii, T., Okada, K., and Iwai, S., *J. Non-Crystallogr. Solids,* 349 (1979).
17. Paramzin, J. M., Zolotovskii, B. P., Krivoruchko, O. P., and Buyanov, R. A., *"Proceedings, VI International Symposium on Heterogeneous Catalysis Sofia,"* Part 2, p. 369 (1987).
18. Chen, F. R., and Guo, X. X., *J. Chem. Soc. Chem. Commun.* **1,** 1682 (1989).
19. Chen, F. R., and Fripiat, J. J., *J. Phys. Chem.*, in press.
20. Che, M, and Tench, A. J., *Adv. Catal.* **32,** 1 (1983).
21. Losee, D. B., *J. Catal.* **50,** 545 (1977).
22. Engelhardt, G., and Michel, D., *"High Resolution Solid-State NMR of Silicates and Zeolites."* Wiley, New York, 1987.
23. Sine bell apodization. Derome, A. E., *"Modern NMR Techniques for Chemistry Research,"* p. 205. Pergamon Press, Elmsford, NY, 1980.
24. Samoson, A., and Lippma, E., *Chem. Phys. Lett.* **134,** 589 (1987).
25. Kentgens, A. P. M., Lemmens, J. J. M., Geurts, F. M., and Veeman, W. S., *J. Mag. Res.* **71,** 62 (1987).
26. Samoson, A., and Lippmaa, E., *J. Mag. Res.* **79,** 255 (1988).
27. Walter, T. H., and Oldfield, E., *J. Phys. Chem.* **93,** 6744 (1989).
28. Knözinger, H., and Ratnasamy, P., *Catal. Rev. Sci. Eng.* **17,** 31 (1978).
29. Hightower, J., and Hall, W. K., *Trans. Faraday Soc.* **66,** 477 (1970).
30. Van Cauwelaert, F. H., and Hall, W. K., *Trans. Faraday Soc.* **66,** 477 (1970).
31. Shannon, R. D., Gardner, K. H., Staley, R. H., Bergeret, G. Gallezot, P., and Auroux, A., *J. Phys. Chem.* **89,** 4778 (1985).